ERJ
Engineering Research Journal
Faculty of Engineering
Menoufiya University

SINGLE SWITCH BOOST DC-DC CONVERTER WITH HIGHER VOLTAGE GAIN

Nerveen M. Tawfik, Mohamed E. Ibrahim, Arafa S. Mansour, and S. S. Shokralla

Electrical Engineering Department, Faculty of Engineering, Menoufia University, Shebin El-Kom (32511), Egypt

ABSTRACT

In this paper, a new approach of DC-DC boost converter has been designed with the aid of an additional inductor, diode and capacitor offering a flexibility in electrical performance and challenging cost problem. The analysis of the modified boost converter is found out an advantage of improving the voltage gain with various choice of loads without any limitations in the duty ratio. The principle operation of the modified boost converter for steady state response in continuous conduction mode is discussed. The performance of the proposed converter is compared to the conventional converter, as the experimental data in the laboratory tests show full agreement with the simulation results.

يقدم هذا البحث تصميم جديد لمنظم تحويل رافع للجهد بإضافة ملف، صمام ثنائي و مكثف و من ثم تقدم المرونة في الأداء الكهربائي و التحدى في حل مشكلة التكلفة. حيث يتميز منظم التحويل المطور بتحسين زيادة الجهد لحالات تغير الأحمال دون قيود فى دورة التشغيل. ويناقش البحث عملية تشغيل منظم التحويل المطور ليعطى الإستجابة المطلوبة فى حالة الإستقرار اثناء وضع التوصيل المستمر. تم المقارنة ما بين أداء منظم التحويل المقترح و منظم التحويل التقليدي حيث أظهرت البيانات التجريبية في الاختبارات المعملية إتفاق كامل مع النتائج النظرية.

Keywords : Boost converter, voltage gain, CCM, duty ratio**.**

1. INTRODUCTION

DC-DC converters are widely used to transform and distribute DC power in systems and instruments including Switch Mode DC-Power Supplies (SMPS) for personal computers, office equipment, spacecraft power systems, laptop computers, industry of telecommunication, dc motor drives and Hybrid Electric Vehicles (HEV) [1]. In practice, supply bus distribution problems, economics, and noise requirements often make DC-DC converter preferable to ensure treatment of poorly unregulated output voltage [2-3].

The conventional boost converter is defined as a step up chopper which converts the unregulated DC input of the power supply (from rectifier or filter or battery or fuel cell, etc.) to a controlled DC output with a desired voltage level. Problems may arise such as high Total Harmonic Distortion (THD), high ripple current, high Electro-Magnetic Interference (EMI), high conduction losses, and high switching stresses [4-6].

A new topology to overcome the previous drawbacks by using bridgeless boost converter, so it presents widespread attention solution for heavy loads (>1kw), doing excellent performance for large-sized flat panel displays. As main drawbacks, EMI begin to increase [7-8], increasing in Common-Mode (CM) noise due to High Frequency (HF) pulsating of charging and discharging of voltage source [9], unacceptable increasing in cost. To keep constant current ripple, the size of boost inductor has been doubled as is needed to facilitate the explanation of large CM choke as a noise [10-11] reducing power density due to large parasitic capacitance between the output bus and ground.

Conventional interleaved boost converter is achievable using two paralleled boost converters operating 180° out of phase with two parallel switches [12-14]. As result, the effective switching frequency is increased by twice value reducing the input current ripple, consequently the input EMI can be smaller. However, the input diode bridge rectifiers is introduced resulting a heat management, so the overall efficiency of previous converter is improved by using high voltage gain interleaved boost converter.

A new topology is modelled for obtaining high voltage gain in Continuous Conduction-Mode (CCM) using a voltage- doubler circuit has been magnetically coupled with an isolated transformer using the high frequency AC link to conventional-interleaved boost converter by adding three magnetic cores [15]. By adding two coupled inductors to the conventional interleaved-boost arrangement resulting higher output voltage with reduced voltage stress across the main switches by increasing the transformer turns-ratio. Low input current ripple and voltage balancing between capacitors are achieved. The main drawback is the limitation of duty cycle, it must be higher than 50%.

Phase shifted semi-bridgeless boost topology presents two-stages approach with cascaded AC-DC and DC-DC converter achieving Power Factor Correction (PFC) [16-17]. It is operating 180° out of phase. Its operation is classified into four sub-sections [18]. It is considered as an attractive solution to overcome the previous subjected problems topologies, so it is convenient application for the front-end AC-DC converter in Plug in Hybrid Electric Vehicle (PHEV). Higher efficiency can be achieved at light loads and low lines which is capable of decreasing the charger size, and the charger cost [19].

Fly-back converter is an isolated DC-DC converter [20]. It is used in both AC-DC and DC-DC conversion with a special method of galvanic isolation between the input and any output. This topology indicates comparison of the parasitic elements on noise at different kinds for resonant converters [21-22] and noise characteristics [23]. The main drawbacks are: high density packaging at the same time with minimum weight of converter, needing soft starting, duty cycle lamination lower than 50% and limitations on continuous and Discontinuous Conduction-Mode respectively (CCM & DCM) [24].

This paper presents a modified boost converter which provides high voltage gain with simple and fast model. This proposed model in conjunction with the various loads can be effectively service the load disturbance, reducing cost, size and heat management problems.

2- Design Analysis of the Conventional DC-DC Boost and the Modified Boost Converter:

2.1 Static Load

First model: Conventional DC-DC Boost Converter

The basic conventional boost converter is look like the transformer, thus the type of this converter must be non-isolated [25].

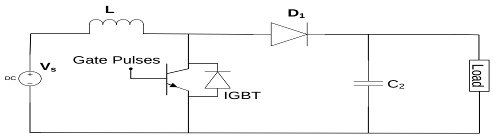

Fig. 1: Conventional DC-DC Boost Converter

In this model as shown in Fig. 1, two stages of this operation can be explained as the following analysis:
Mode (1); as shown in Fig. 1(a). Current passes from the input source V_s through the input inductance L and IGBT, an energy is stored in the inductor's magnetic field observing no current through D_1, and the load current is supplied by charging of C_2.
Assume: a pure inductance and negligible resistance.

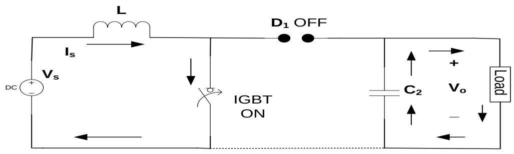

Fig. 1: (a) Mode (1), the switch is closed

$$V_S = L\frac{dI_s}{dt} \tag{1}$$

$$\frac{dI_s}{dt} = \frac{\Delta I_s}{\Delta t} = \frac{\Delta I_s}{kT} = \frac{V_s}{L} \tag{2}$$

Mode (2); as shown in Fig. 1(b). The EMF is reversed immediately making drop in the inductor current which results adding an inductor voltage to the source voltage and the source current I_s due to this recent boosted voltage is passed from the source through L , D_1 and the load as well as recharging C_2.

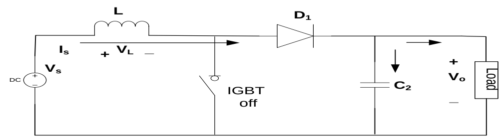

Fig. 1: (b) Mode (2), the switch is opened

$$V_o = V_s + V_L \tag{3}$$

$$\frac{dI_s}{dt} = \frac{\Delta I_s}{\Delta t} = \frac{\Delta I_s}{(1-k)T} = \frac{(V_s - V_o)}{L} \tag{4}$$

At steady state operation in continuous conduction-mode:
The current at the start and the end of a period T will not change, assuming no voltage drop across the switch.

$$(\Delta i_L)_{closed} + (\Delta i_L)_{opened} = 0 \tag{5}$$

$$V_s kT + (V_s - V_o)(1-k)T = 0 \tag{6}$$

$$V_o = \frac{V_S}{(1-k)} \tag{7}$$

For the lossless circuit, the power balance ensures:

$$\frac{I_o}{I_s} = (1-k) \tag{8}$$

Second model: Proposed Modified DC-DC Boost Converter

In this model as shown in Fig. 2, by adding a new RL branch, capacitor C_1, and diode D_2 is used for not reversing the direction of current directly to the load. In fact, L_1 is chosen to have a small value as its function omits the very high current spikes during charging C_1.

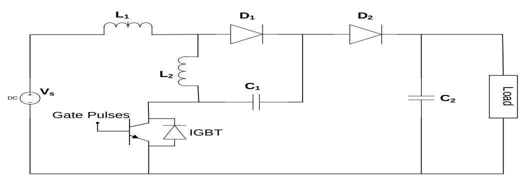

Fig. 2: Modified DC-DC Boost Converter

The proposed converter uses a taped inductor (or three terminals inductor) instead of using two terminals inductor.

Two stages of this operation can be explained as the following analysis emphasizing higher voltage gain:

Mode (1); when the power switch (S) is turned on, capacitor C_1 is charged from the DC supply through the inductor portion L_1 and diode D_1 with the polarity as shown in Fig. 2(a).

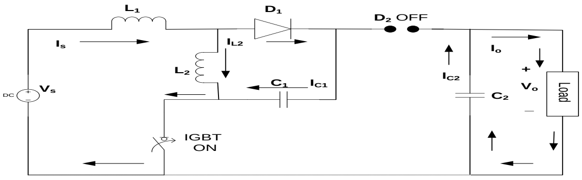

Fig. 2: (a) Mode (1), the switch is closed

$$V_s = L\frac{\Delta I}{t_1} = L\frac{I_2 - I_1}{t_1} \quad (9)$$

Then, $$t_1 = L\frac{\Delta I}{V_s} \quad (10)$$

Mode (2); when the switch S is turned off, as shown in Fig. 2 (b). The total inductor voltage reverses its polarity in a direction that enhances the supply voltage. Therefore, capacitor C_2 is charged with a voltage equal to the summation of supply, total inductor, and capacitor C_1 voltages. At the same time, the current rises linearly in the inductor (L_1+L_2) allowing the inductor to store energy.

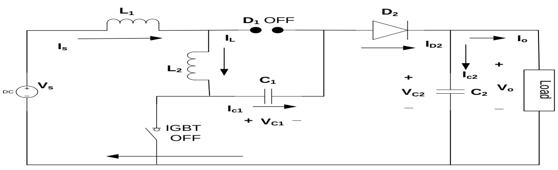

Fig. 2: (b) Mode (2), the switch is opened

$V_o = V_{C2} = V_s + V_L + V_{C1}$ (11)

$V_L = (V_o - 2V_s)$ (12)

$$V_L = L\frac{\Delta I}{t_2} = L\frac{I_2 - I_1}{t_2} \quad (13)$$

Then, $$t_2 = L\frac{\Delta I}{(V_O - 2V_s)} \quad (14)$$

From equations (10) and (14), the output voltage is:

$$V_O = V_S\,\frac{(2-k)}{(1-k)} \quad (15)$$

For the lossless circuit, the power balance ensures:

$$I_s = I_o\frac{(2-k)}{(1-k)} \quad (16)$$

Fig. 3 shows the waveforms of the proposed DC-DC boost converter assuming ideal elements during the period T, where (T= t_{on} + t_{off}).

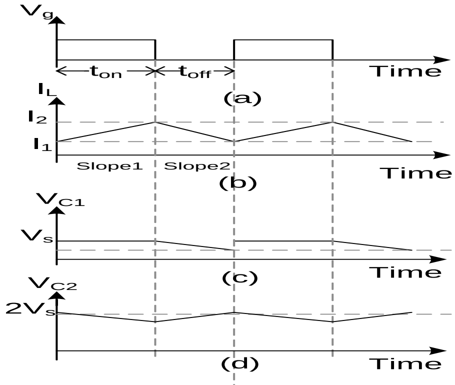

Fig. 3 Waveforms of the proposed DC-DC boost converter assuming ideal elements, (a) Gate Pulses, (b) Inductor L current, (c) Capacitor C_1 voltage, and (d) Capacitor C_2 voltage.

Accordingly, the relationship between the voltage gain and the duty ratio becomes significant to maintain a good work of the modified boost converter higher than the conventional boost converter. The voltage conversion ratio as a function of the duty cycle (k) for an ideal boost converter in CCM is deduced from the previous equations (7) and (15). Figure 4 indicates the output voltage control which is depending on variable values of duty cycle (k) with respect to time (Sec.).

The duty ratio of conventional boost converter:

$$D_1 = \frac{V_O}{V_S} \quad (17)$$

$$D_1 = \frac{1}{(1-k)} \quad (18)$$

The duty ratio of modified boost converter:

$$D_2 = \frac{V_O}{V_S} \quad (19)$$

$$D_2 = \frac{(2-k)}{(1-k)} \quad (20)$$

From the equations (18) and (20) obtaining the following note:

$D_2 > D_1$ (21)

So the modified boost converter has high voltage gain providing better performance than the conventional one and reducing the switch voltage stress.

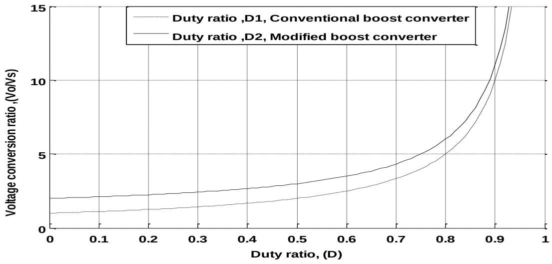

Fig. 4: Effect of duty ratio (D) on voltage gain (V_o/V_s)

2.2 Dynamic Load

The fundamental concept of the converter fed a universal DC motor in which the accurate control of motion where placing an object in the exact desired location with the exact possible amount of force and torque at the correct exact time which is essential for efficient traction system [26]. The schematic diagram for a DC series motor equivalent circuit is shown in Fig. 5:

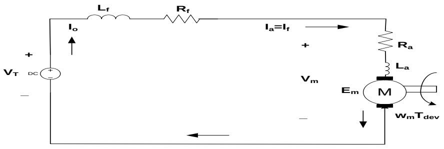

Fig. 5: DC series motor equivalent circuit

…The dynamic equations describe the electro-mechanical behavior are given that the electrical equilibrium equation is applying by Kirchhoff voltage law to the equivalent circuit:

$$V_T = E_m + R_t I_o + L_t \frac{dI_o}{dt} \tag{22}$$

Where, V_T is the voltage applied to the armature terminals, E_m is the induced EMF, R_t is the total series resistance; ($R_t = R_f + R_m$), I_o is the current through the windings and L_t is the total series inductance; ($L_t = L_f + L_m$).

The relation of induced voltage E_m with magnetic flux ϕ and angular speed ω :

$$E_m = K_m \phi \omega_m(t) \tag{23}$$

where, K_m is a motor constant.

The electromagnetic torque developed by the DC motor: $T_{em}(t) = K_m \phi I_o$ (24)

The torque balance equation is:

$$T_{em}(t) = T_L + B\omega + J\frac{d\omega}{dt} \tag{25}$$

The magnetic flux and the windings current are related through the machine's magnetization curve.as follows:

$$\phi = F(I_o) \tag{26}$$

where, function $F(I_o)$ in general includes saturation and hysteresis effects

The magnetic flux actually is an intermediate variable for the calculation of E_m:

$$E_m = K_m \omega_m I_o \tag{27}$$

From equation (24) and (26) obtaining that the torque.

$$T_{em} = K_m I_o^{\,2} \tag{28}$$

Two stages of this dynamic operation can be explained as the following analysis emphasizing higher voltage gain as shown in Figs. 5(a) and 5(b):

The differential equations describing mode (1) are written as follows (resistances of coils are considered):

$$V_m = V_{C2} \tag{29}$$

$$V_S = L_1\frac{dI_s}{dt} + L_2\frac{dI_L}{dt} + R_1 I_s + R_2 I_L \tag{30}$$

$$V_S = \frac{1}{C_1}\int I_{C1}dt \tag{31}$$

$$V_{C2} = \frac{1}{C_2}\int I_O dt \tag{32}$$

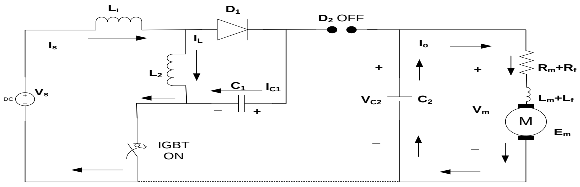

Fig. 5(a): Mode (1), the switch is closed

The differential equations describing mode (2) are written as follows (resistances of coils are considered):

$$V_S = (R_1 + R_2)I_s + (L_1 + L_2)\frac{dI_s}{dt} + \frac{1}{C_1}\int I_s dt + \frac{1}{C_2}\int I_{C2}dt \tag{33}$$

$$I_O = I_{D2} - I_{C2} \tag{34}$$

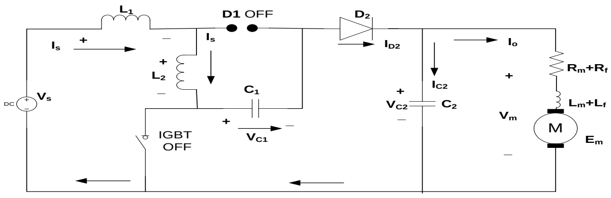

Fig. 5(b): Mode (2), the switch is opened

3- Simulation Results

The model of the proposed boost converter is compared with the conventional one to verify the best behavior of the first one under steady state condition. Two distinct loads are considered: static load (purely resistive load (R load), an inductive load (R-L load)) and dynamic load (a universal motor). The MATLAB simulation of an open loop speed control is considered. The measured parameters of the conventional and the proposed boost converters are indicated in Table 1.

Table 1: The parameters of the conventional and modified converters

Item	Symbol	Value
Parameters of the conventional converter		
Resistance of coil Portion 1	R_1	2.8 Ω
Inductance of coil Portion 1	L	3 mH
Parameters of the proposed converter		
Resistance of coil Portion 1	R_1	0.1 Ω
Inductance of coil Portion 1	L_1	0.1 mH
Resistance of coil Portion 2	R_2	2.8 Ω
Inductance of coil Portion 2	L_2	3 mH
Capacitor C_1 Capacitance	C_1	47 µF
Common data for both converters		
Capacitor C_2 Capacitance	C_2	500 µF
Voltage source	V_s	100 v
Switching frequency	$f_{s=}(1/T)$	1 KHZ

3-1 R-Load

The simulation results for purely resistive load (R_L= 50 Ω) of the input currents, output currents, and output voltages at different values of duty ratio K (0.2, 0.5, and 0.8) are presented in Figs. 6, 7, and 8 respectively.

Figure 6 shows the simulation results at duty cycle 0.2. The input currents of both of the conventional and modified boost converters are shown in Figs. 6(a) and 6(b) respectively. Fig. 6(c) shows the output current of the modified boost converter exceeds over the conventional one (2.3A to 3.8A). Fig. 6(d) shows the output voltage of the modified boost converter exceeds over the conventional one by 56%.

Figure 7 shows the simulation results at duty cycle 0.5. The input currents of both of the conventional and modified boost converter are shown in Figs. 7(a) and 7(b), respectively. Fig. 7(c) shows the output current of the modified boost converter exceeds over the conventional one (3.2A to 4.6A). Fig. 7(d) shows the output voltage of the modified boost converter exceeds over the conventional one by nearly 44%.

Figure 8 shows the simulation results at duty cycle 0.8. The input currents of both of the conventional and modified boost converters are shown in Figs. 8(a) and 8(b), respectively. Fig. 8(c) shows the output current of the modified boost converter exceeds over the conventional one (4.1A to 4.8A). Fig. 8(d) shows the output voltage of the modified boost converter exceeds over the conventional one by nearly 17%.

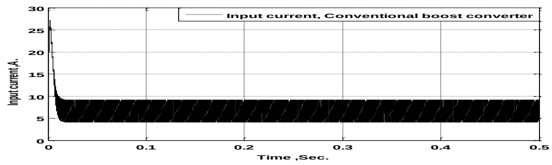

(a)

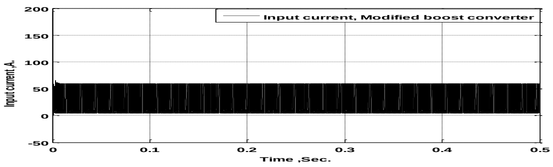

(b)

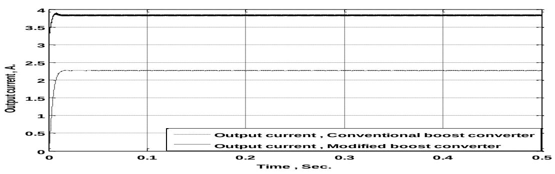

(c)

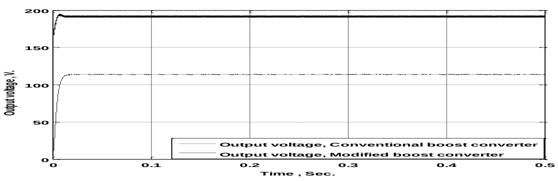

(d)

Fig. 6: Simulation results of the (a) Conventional boost converter's input current , (b) Modified boost converter 's input current, (c) output current, and (d) output voltage at R = 50 ohm and K = 0.2.

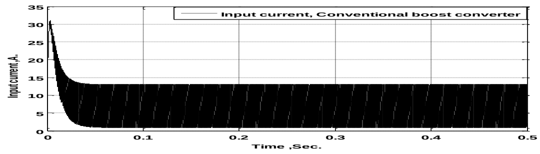

(a)

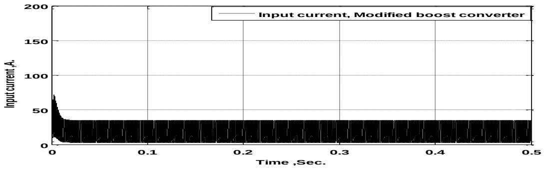

(b)

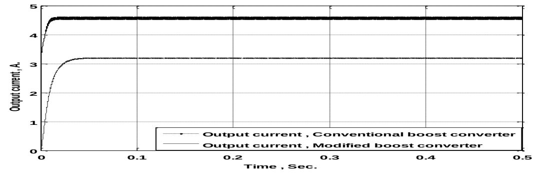

(c)

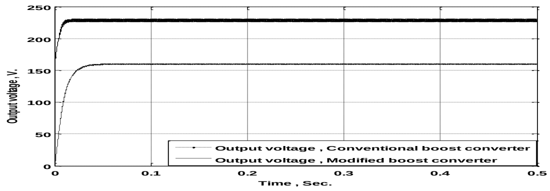

(d)

Fig. 7: Simulation results of the (a) Conventional boost converter's input current , (b) Modified boost converter 's input current, (c) output current, and (d) output voltage at R = 50 ohm and K = 0.5.

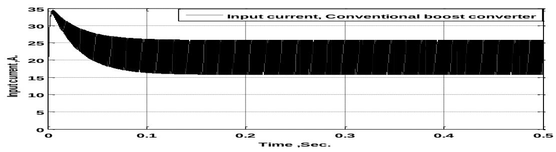

(a)

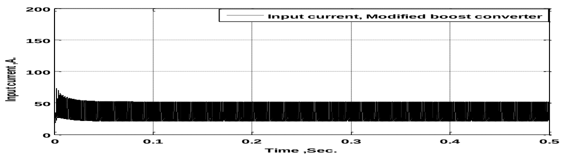

(b)

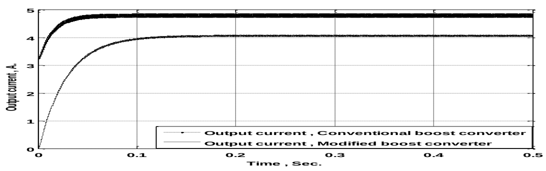

(c)

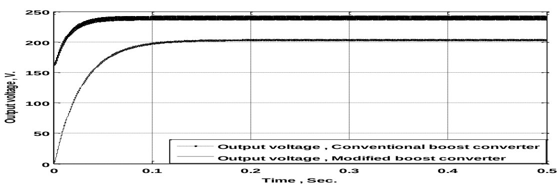

(d)

Fig. 8: Simulation results of the (a) Conventional boost converter's input current , (b) Modified boost converter 's input current, (c) output current, and (d) output voltage at R = 50 ohm and K = 0.8.

3-2 R-L Load

The simulation results for an inductive load (R_L= 50 Ω and L_L=1 mH) of input currents, output currents, and output voltages at different values of duty ratio k (0.2, 0.5, and 0.8) are presented in Figs. 9, 10 and 11, respectively. The observed results are nearly typical to the results of R load.

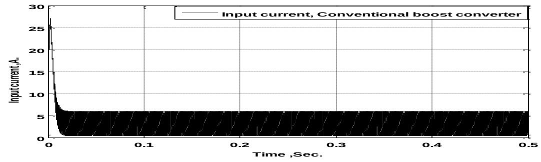

(a)

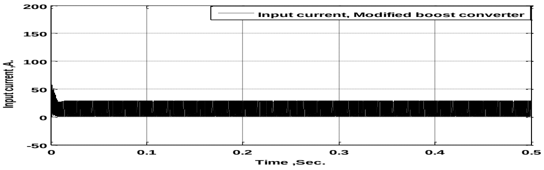

(b)

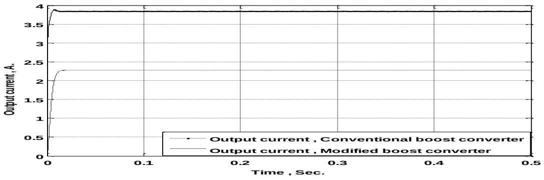

(c)

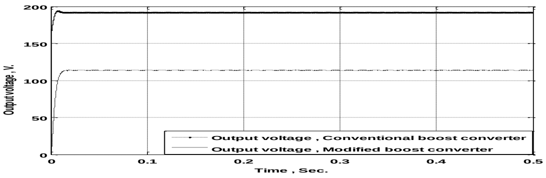

(d)

Fig. 9: Simulation results of the (a) Conventional boost converter's input current , (b) Modified boost converter 's input current, (c) output current, and (d) output voltage at R_L= 50 ohm, L_L= 0.01H and K= 0.2.

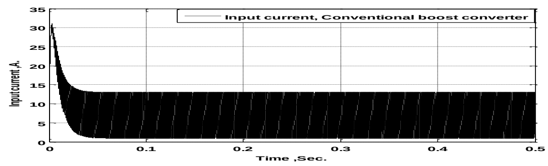

(a)

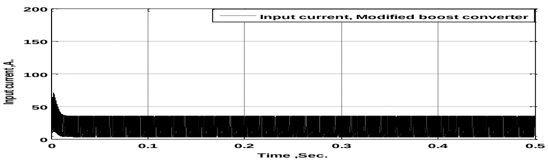

(b)

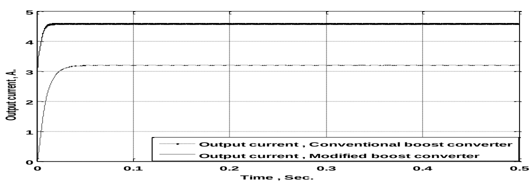

(c)

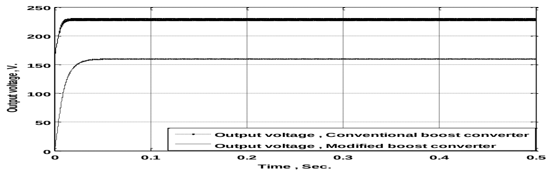

(d)

Fig. 10 Simulation results of the (a) Conventional boost converter's input current , (b) Modified boost converter 's input current, (c) output current, and (d) output voltage at R_L = 50 ohm, L_L = 0.01 H and K= 0.5.

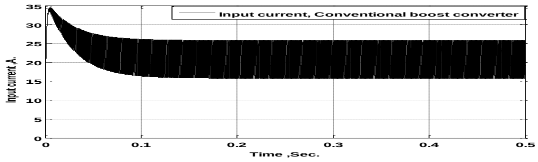

(a)

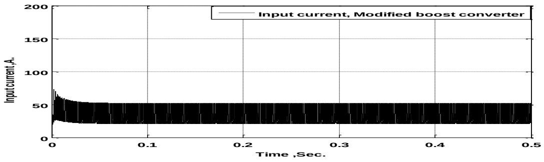

(b)

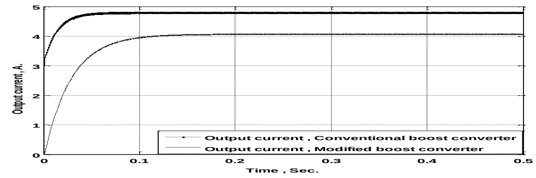

(c)

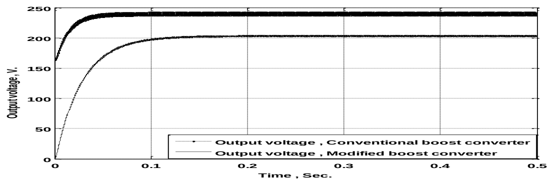

(d)

Fig. 11 Simulation results of the (a) Conventional boost converter's input current , (b) Modified boost converter 's input current, (c) output current, and (d) output voltage at R_L= 50 ohm, L_L= 0.01 H and K= 0.8.

3-3 Dynamic Load

In this case, the load torque is equal to the full load, in which the universal motor parameters are indicated in Table 2.

The simulation results of the input current in case of the conventional boost converter and the modified boost converter, output current and output voltage at different values of the duty cycle K (0.2, 0.5 and 0.8) are presented in Figs. 12, 13 and 14, respectively.

It can be seen from Figs. 12(d), 13(d) and 14(d) that the output voltage of the modified boost converter exceeds over the conventional one by approximately 70%, 32% and 25%, respectively.

Table 2: Universal motor parameters

Item	Symbol	Value
Armature & Field resistances	$R_a = R_f$	2.581 Ω
Armature & Field inductances	$L_a = L_f$	0.028 H
Frequency	F	50 Hz
Motor constant	K_m	0.5161V/(Rad/Sec.)
Moment of inertia	J	0.02215 $Kg.m^2$
Viscous friction constant	B	0.002953 N.m/Rad/Sec.

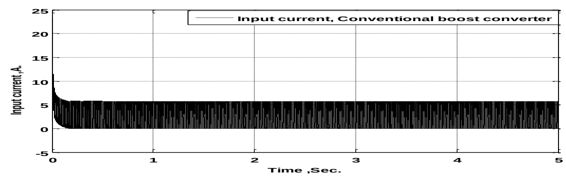

(a)

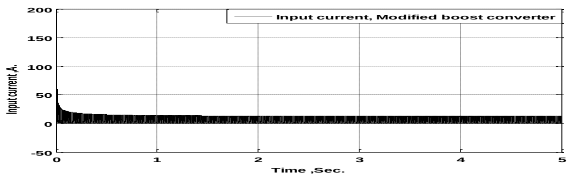

(b)

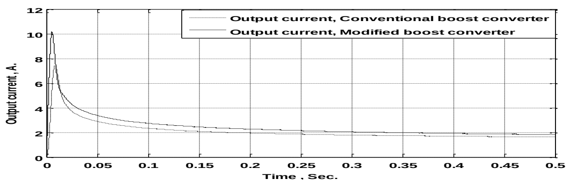

(c)

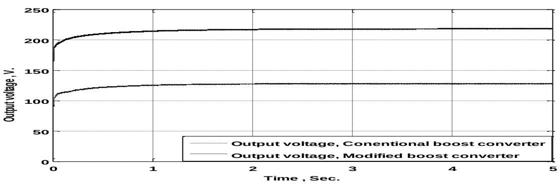

(d)

Fig. 12 Simulation results of the (a) Conventional boost converter's input current, (b) Modified boost converter 's input current, (c) output current, and (d) output voltage at K = 0.2.

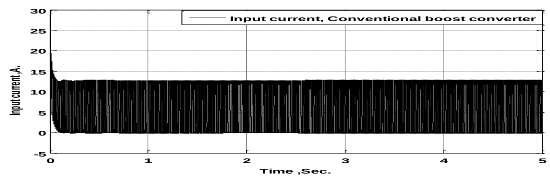

(a)

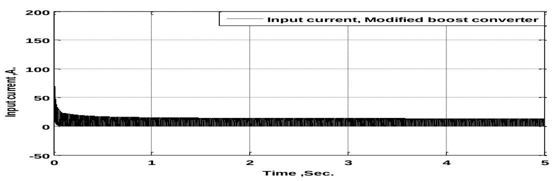

(b)

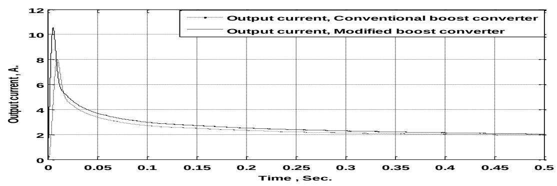

(c)

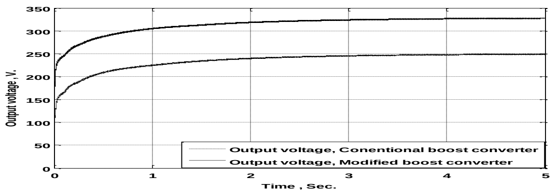

(d)

Fig. 13 Simulation results of the (a) Conventional boost converter's input current, (b) Modified boost converter 's input current,(c) output current, and (d) output voltage at K = 0.5.

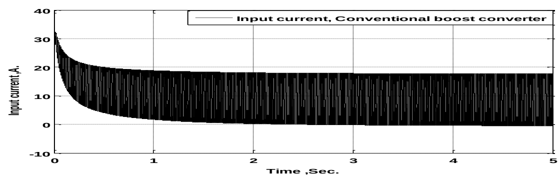

(a)

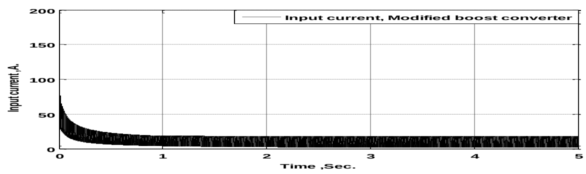

(b)

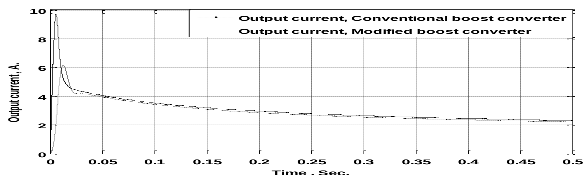

(c)

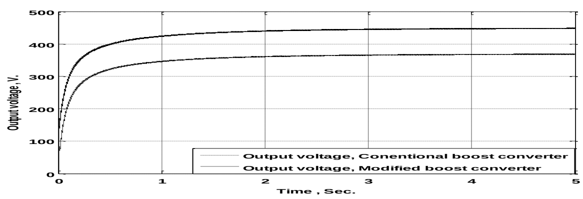

(d)

Fig. 14 Simulation results of the (a) Conventional boost converter's input current, (b) Modified boost converter 's input current, (c) output current, and (d) output voltage K = 0.8.

In the previous different load cases, the rise time of both of the output voltages and output currents of the modified boost converter are lower than it of both the output voltages and output currents of the conventional one. It can be seen that the supply current drawn from the source with the proposed converter is higher than it for the conventional converter. Those results are logic as the proposed converter gives a higher voltage gain.

4- Experimental Results

To validate the proposed design, an experimental circuit is built. The designed circuit parameters are chosen as Table 3 and an IGBT (G4PC50W) is used. The results are obtained by using a storage oscilloscope at which data can be collected by a USB as samples. Then the collected data are plotted using MATLAB program.

Figures 15 to 17 show the experimental results of supply, capacitor C_1, and output voltages of the proposed converter at duty cycles 0.5, 0.64 and 0.27, respectively when feeding a purely resistive load of 150 Ω. These figures illustrate the proposed idea. The reason for supply voltage distortion is a high internal impedance of supply.

Table 3: The parameters of the conventional and modified converters.

Item	Symbol	Value
Inductor Portion 1 Inductance	L_1	1 mH
Inductor Portion 2 Inductance	L_2	3 mH
Capacitor C_1 Capacitance	C_1	96 µF
Capacitor C_2 Capacitance	C_2	1650 µF
Switching frequency	f_s=(1/T)	1.5 KHZ

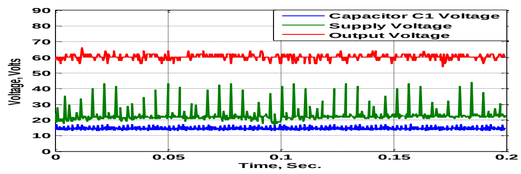

Fig. 15 Measured Capacitor C_1, Supply, and Output Voltages of the proposed Converter, Resistive Load (R_L=150 Ω), Duty Ratio = 0.5, Switching Frequency = 1500 Hz.

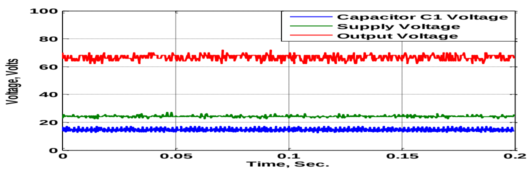

Fig. 16 Measured Capacitor C_1, Supply, and Output Voltages of the proposed Converter, Resistive Load (R_L=150 Ω), Duty Ratio = 0.64, Switching Frequency = 1500 Hz.

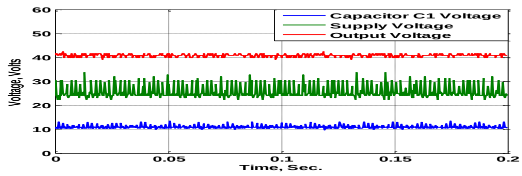

Fig. 17 Measured Capacitor C_1, Supply, and Output Voltages of the proposed Converter, Resistive Load (R_L=150 Ω), Duty Ratio = 0.27, Switching Frequency = 1500 Hz.

Also, Figs. 18 to 20 show the experimental results of supply, and output voltages of the conventional DC-DC boost converter of the same parameters at duty cycles of 0.5, 0.64, and 0.27 respectively when feeding a purely resistive load of 150 Ω.

Looking to Figs. 13 to 18, the proposed converter gives a higher voltage gain as compared to conventional especially at low duty ratios.

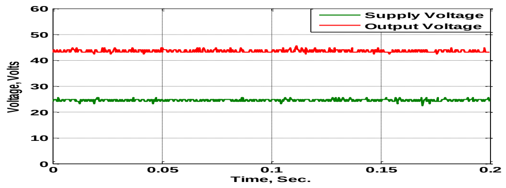

Fig. 18 Measured Supply, and Output Voltages of the Conventional DC-DC Boost Converter, Resistive Load (R_L=150 Ω), Duty Ratio = 0.5, Switching Frequency = 1500 Hz.

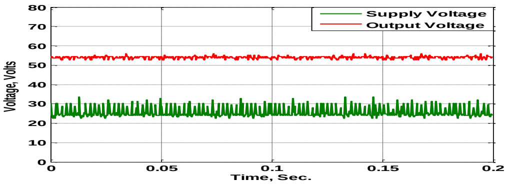

Fig. 19 Measured Supply, and Output Voltages of the Conventional DC-DC Boost Converter, Resistive Load (R_L=150 Ω), Duty Ratio = 0.64, Switching Frequency = 1500 Hz.

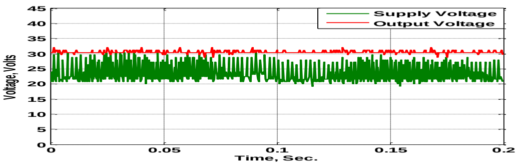

Fig. 20 Measured Supply, and Output Voltages of the Conventional DC-DC Boost Converter, Resistive Load (R_L=150 Ω), Duty Ratio = 0.27, Switching Frequency = 1500 Hz.

5- Conclusions

The field of study in this paper has been demonstrated the technical aspects of the proposed modified boost converter at the same time of a simple design needing only one switch. This new approach has been contributed a new knowledge to reveal the drawbacks of the conventional converter. It can be employed for any value of the duty cycle without any limitations. The main argument is appropriate by the experimental tests and the simulated results to elaborate on the impact of a comparison between the conventional boost converter and the modified boost one. A good manner of the modified boost converter has been predicted the behavior of performance on the voltage gain at continuous conduction-mode and instantaneously quicker than the conventional one at steady state condition.

REFERENCES

[1] M. Ehsani, Y. Gao and A. Emadi, "Modern Electric, Hybrid Electric and Fuel Cell Vehicles: Fundamentals, Theory and Design", 2nd edition, Chemical Rubber Company (CRC Press), 2009.

[2] K. Tachibana, T. Tsuboi, and S. Kariya, "Harmonic Currents in Catenary Systems from Chopper Control", IEEE Transactions on Industry Applications, Vol. 8,No. 2, pp. 203-210, March 1972.

[3] S. B. Dewan, G. S. Dang, and N. H. Nicholson, "A Fast Response DC Chopper", In Annual Conference Records IEEE, IAS, pp. 922-929, 1975.

[4] Y. Murai, T. Kubota and Y. Kawase, "Leakage current reduction for a high-frequency carrier inverter feeding an induction motor", IEEE Transactions on Industry Applications, Vol. 28, No.4, pp.858-863, July/August 1992.

[5] T. Shimizu and G. Kimura, "High-frequency leakage current reduction based on a common-mode voltage compensation circuit", 27th Annual IEEE Power Electronics Specialists Conference (PESC), Baveno, Italy, Vol. 2 ,pp. 1961-1967, June 1996.

[6] S. Shimizu, G. Kimura, and J. Hirose," High frequency leakage current caused by the transistor module and its suppression technique", IEEJ Transactions on Industry Applications, Japan, Vol. 116, No-7, pp. 758-766, January 1996.

[7] L. Huber, Y. Jang, and M. M. Jovanovic, "Performance Evaluation of Bridgeless PFC Boost Rectifiers", IEEE Transactions on Power Electronics, Vol. 23, pp. 1381-1390, 2008.

[8] P. Kong, S. Wang, and F.C. Lee, "Common Mode EMI Noise Suppression for Bridgeless PFC Converter", IEEE Transactions on Power Electronics,Vol.23, No. 1, pp. 291-297, January 2008.

[9] M. Gopinath, Prabakaran, and S. ramareddy, "A Brief Analysis on Bridgeless boost PFC Converter", Second IET International Conference on Sustainable Energy and Intelligent Systems (SEISCON), Chennai, India, pp. 242-246, July 2011.

[10] H. Ye, Z. Yang, J. Dai, C. Yan, X. Xin, and J. Ying, "Common Mode Noise Modeling and Analysis of Dual Boost PFC circuit", 26th Annual International Conference of the IEEE Telecommunications Energy, (INTELEC), Chicago, IL, USA, pp. 575-582,September 2004.

[11] Lu Bing, Ron Brown and Marco Soldano, "Bridgeless PFC Implementation Using One Cycle control Technique", 20th Annual Conference of the IEEE Applied Power Electronics and Exposition (APEC), Austin, TX, USA, Vol. 2, pp.812-817, March 2005.

[12] H. Kosai , S. McNeal, A. Page, B. Jordan, J. Scofield and B. Ray, "Characterizing the effects of inductor coupling on the performance of an interleaved boost converter", 29th Annual Passive Components and Exhibition, CARTS, USA, pp. 237–251, March 2009.

[13] X. Huang, X. Wang, T. Nergaard, J. Lai, X. Xu, and L. Zhu, "Parasitic ringing and design issues of digitally controlled high power interleaved boost converters", IEEE Transactions Power Electronics, Vol.19, No. 5, pp. 1341–1352, September 2004.

[14] Y. Xie and H. Tian, "Characteristics analysis of two-channel interleaved boost converter with integrated coupling inductors", 37th Annual IEEE Power Electronics Specialists Conference (PESC), pp. 1-6, June 2006.

[15] H. Kosai, S. McNeal, B. Jordan, J. Scofield, B. Ray and Z. Turgut, "Coupled Inductor Characterization for High Performance Interleaved Boost Converter", IEEE Transactions on magnetics, Vol. 45, No. 10, pp. 4812-4815, October 2009.

[16] L. Petersen, and M. Andersen, "Two-Stage Power Factor Corrected Power Supplies: The Low Component-Stress Approach", 17th Annual Conference of the IEEE Applied Power Electronics and Exposition (APEC), Dallas, TX, USA, Vol. 2, pp. 1195-1201, March 2002.

[17] B. Singh, B.N. Singh, A. Chandra, K. Al-Haddad, A. Pandy and D. P. Kothari, "A Review of Single-Phase Improved Power Quality AC-DC Converters", IEEE Transactions on Industrial Electronics, Vol. 50, No. 5, pp. 962-981, October 2003.

[18] F. Musavi, M. Edington, W. Eberle and W. G. Dunford, "Evaluation and Efficiency Comparison of Front End AC-DC Plug-in Hybrid Charger Topologies", IEEE Transactions on Smart Grid, Vol. 3, No. 1, pp. 413-421, March 2012.

[19] Y. Lee, A. Khaligh and A. Emadi, "Advanced Integrated Bidirectional AC-DC and DC-DC Converter for Plug-In Hybrid Electric Vehicles", IEEE Transactions on Vehicular Technology, Vol. 58, No. 8, pp. 3970-3980, October 2009.

[20] N. Mohan, T. M. Undeland and W. P. Robbins, "Power Electronics: Converters, Applications and Design", 3rd edition, John Wiley & Sons, 2003.

[21] K. H. Liu, R. Oruganti and F. C. Lee, "Resonant switches-topologies and characteristics", 16th Annual IEEE Power Electronics Specialists Conference (PESC), pp.106-116, June 1985.

[22] K. H. Liu and F.C. Lee, "zero-voltage switching technique in DC/DC converter", IEEE Transactions on Power Electronics, Vol. 5, No. 3, pp. 293-304, July 1990.

[23] A. Ostadi, X. Gao, and G. Moschopoulos, "Circuit properities of Zero-Voltage-Transition PWM converters", Journal of power electronics. Vol. 8, No. 1, pp. 35-50, January 2008.

[24] L. Hsiu, M. Goldman, A. F. Witulski, W. Kerwin, and R. Carlsten, "Characterization and comparison of noise generation for quasi-resonant and pulse-width modulated converters", 22nd Annual IEEE Power Electronics Specialists Conference (PESC), Cambridge, MA, USA, pp.504-509, June 1991.

[25] X. Dehong, J. Zhang, W. Chen, J. Lin and F. C. Lee, "Evaluation of output filter capacitor current ripples in single phase PFC converters", in Proceedings of IEEE Power Conversion Conference (PCC), Osaka, Japan, Vol. 3, pp. 1226-1231, April 2002.

[26] S. L. Alerich, and W. N. Herman, "Industrial motor control", Delmar Publishers, Fourth Edition, 1999.